Published in final edited form as:
Connect Tissue Res. 2008 ; 49(6): 391–400. doi:10.1080/03008200802325060.

Transgenic Overexpression of Gremlin Results in Developmental Defects in Enamel and Dentin in Mice

Kanako J. Nagatomo,
Department of Materials Science and Engineering, University of Washington, Seattle, Washington, USA

Kevin A. Tompkins,
Department of Materials Science and Engineering, University of Washington, Seattle, Washington, USA

Hanson Fong,
Department of Periodontics, School of Dentistry, University of Washington, Seattle, Washington, USA

Hai Zhang,
Department of Restorative Dentistry, School of Dentistry, University of Washington, Seattle, Washington USA

Brian L. Foster,
Department of Materials Science and Engineering, University of Washington, Seattle, Washington, USA; Department of Oral Biology, School of Dentistry, University of Washington, Seattle, Washington, USA

Emily Y. Chu,
Department of Materials Science and Engineering, University of Washington, Seattle, Washington, USA; Department of Oral Biology, School of Dentistry, University of Washington, Seattle, Washington, USA

Ayu Murakami,
Department of Materials Science and Engineering, University of Washington, Seattle, Washington, USA

Lisa Stadmeyer,
Department of Research, Saint Francis Hospital and Medical Center, Hartford, Connecticut, USA

Ernesto Canalis, and
Department of Research, Saint Francis Hospital and Medical Center, Hartford, Connecticut, USA; University of Connecticut School of Medicine Farmington, Connecticut, USA

Martha J. Somerman
Department of Materials Science and Engineering, University of Washington, Seattle, Washington, USA; Department of Oral Biology, School of Dentistry, University of Washington, Seattle, Washington, USA

Abstract

Address correspondence to Martha J Somerman, 1959 NE Pacific Box 357444 B-127 Health Sciences Seattle, WA98105 USA. somerman@u.washington.edu.

Declaration of Interest: The authors report no conflicts of interest. The authors alone are responsible for the content and writing of the paper.

Bone morphogenetic proteins (BMPs) and BMP antagonists play a crucial role in the regulation of tooth development. One of the BMP extracellular antagonists, gremlin, is a highly conserved 20.7-kDa glycoprotein. Previously, researchers reported that transgenic mice overexpressing gremlin under the control of the osteocalcin promoter (gremlin OE) exhibit a skeletal phenotype and tooth fragility. To further define the tooth phenotype, teeth and surrounding supporting tissues, obtained from gremlin OE at ages of 4 weeks, 2 months, and 4 months, were examined. The histological results demonstrate that gremlin OE exhibit an enlarged pulp chamber with ectopic calcification and thinner dentin and enamel compared with wild-type control. *In vitro* studies using murine pulp cells revealed that gremlin inhibited BMP-4 mediated induction of *Dspp*. These data provide evidence that balanced interactions between BMP agonists/antagonists are required for proper development of teeth and surrounding tissues. It is clear that these interactions require further investigation to better define the mechanisms controlling tooth root formation (pulp, dentin, cementum, and surrounding tissue) to provide the information needed to successfully regenerate these tissues.

Keywords

Gremlin; BMP; Agonist; Antagonist; Dentin; Regeneration

INTRODUCTION

Bone morphogenetic proteins (BMPs) belong to the transforming growth factor (TGF)-β superfamily of secreted signaling molecules [1–4]. In addition to their ability to induce ectopic bone formation [5], BMPs have widespread signaling functions in skeletal development and in maintenance of bone homeostasis [1]. Proper expression of BMPs and BMP antagonists are crucial for normal tooth development [2–4,6].

BMP-2, -4, and -7 are considered key signals that participate in epithelial-mesenchymal interactions during tooth development [7]. Detailed studies have mapped the temporospatial expression patterns of BMP-2,-4, and -7 during tooth development using the techniques of in situ hybridization and immunohistochemistry [8–17]. Briefly, at initiation of murine tooth development (E10–12), BMP-2 is expressed in the dental lamina, while BMP-4 is expressed in the epithelium and mesenchyme. As tooth development proceeds to the bud stage (E12–13), BMP-4 expression shifts completely to the mesenchyme, while BMP-2 and -7 are expressed in dental epithelium [8,11,16]. During the cap stage (E14–15), BMP-4 is expressed in the enamel knot, which is reported to be a signaling center regulating odontoblast differentiation [15], and in the dental mesenchyme. At this time, expression of BMP-2 and -7 spreads from the enamel knot to the neighboring inner dental epithelium. At the bell stage (E16–19), presumptive ameloblasts express BMP-4, and odontoblasts express BMP-2, -4, and -7 [8–13].

During root formation, BMP-4 is expressed in pre-odontoblastic cells and throughout cells within the pulp, while BMP-2 and -7 are expressed in early odontoblasts. As odontoblasts differentiate further and start to secrete a dentin matrix, BMP-4 expression is markedly downregulated. In contrast to BMP-2, -4, and -7, BMP-3 is a BMP antagonist, able to interfere with the binding of activin and BMP-4 to activin type I receptor without activating R-smads [18,19].

Strong BMP-3 expression is detected in cementoblasts found along the root-forming molars as well as in the dental follicle/periodontal ligament region [17]. BMP-3 overexpressing mice under the control of collagen type I promoter exhibit enlarged pulp chambers, widened periodontal ligament, and increased mobility of teeth with malocclusion [20]. This suggests

BMP-3 has an important role in the maintenance of the soft tissues, i.e., pulp tissue and periodontal ligament.

In vitro, recombinant human BMP-2 (rhBMP-2) has been shown to induce both bovine and human adult pulp cells to differentiate into odontoblasts [21–23]. Beads soaked in rhBMP-2 and -4 also stimulate odontoblast differentiation in organ cultures of murine dental papilla cells [24]. Moreover, rhBMP-2, -4, and -7 are capable of inducing dental pulp cells to form reparative/regenerative dentin in vivo [25–29].

Extracellular antagonists of BMPs include gremlin, noggin, chordin, the DAN/Cerberus family of genes/proteins, ectodin, follistatin, and follistatin-related gene (FLRG), ventroptin, and twisted gastrulation (Tsg) [1]. These antagonists prevent BMP signaling by binding BMP, thereby precluding BMP from binding to receptors on the cell surface. Each extracellular antagonist binds specific members of the BMP superfamily with different affinities.

Transgenic mice overexpressing follistatin, ectodin, and noggin exhibit tooth phenotypes [2, 3,6], indicating the importance of the interactions between BMPs and their antagonists for normal tooth development. Further, studies mapping the temporospatial expression of these antagonists indicate that follistatin is a key regulator of enamel, dentin, and cementum formation. It is less clear as to the role of the other antagonists. For example, noggin and gremlin expression have been detected in dental mesenchyme at E14 selectively [30].

The BMP antagonist, gremlin, is the focus of our studies here. Gremlin is a member of Dan/Cerberus family, a highly conserved 20.7-kDa glycoprotein and was originally isolated in Xenopus embryos as an anti-BMP dorsalizing agent [31]. Gremlin binds and blocks the actions of BMP-2, -4, and -7 and is expressed in osteoblasts [1]. Studies by Pereira et al. [32] indicated that BMP signaling induces gremlin expression, suggesting a feedback mechanism in the regulation of BMP antagonists and agonists [33]. Beyond gremlin's extracellular binding to BMPs, gremlin binds to a BMP-4 precursor protein intracellularly, preventing production and secretion of mature BMP-4 protein, resulting in the downregulation of BMP-4 ligand signaling. This mechanism has been suggested to have a more potent antagonistic effect on BMPs than the extracellular binding of BMPs by gremlin [34].

Mice overexpressing gremlin under the control of the osteocalcin promoter exhibit a decrease in body size, spontaneous fractures, modeling defects of long bones, and severe osteopenia [35]. At birth, gremlin OE mice are indistinguishable from wild-type controls, but by 1.5–2 weeks of age, they appear smaller. At 4.5 weeks, the body weight is reduced by approximately 35%. Interestingly, Gazzerro et al. [35] also noted abnormalities in tooth development; lower incisors which erupted normally but fractured, so that upper incisors grew unopposed, interfering with proper occlusion.

Based on these findings, the studies presented here were performed to further characterize the tooth phenotype in gremlin OE mice.

MATERIALS AND METHODS

Gremlin Transgenics

Gremlin transgenic mice were generated to direct gremlin expression under the control of the rat osteocalcin promoter, as previously reported [35]. Briefly, founder transgenic mice were bred to wild-type CD-1 mice to generate individual transgenic lines. First-generation heterozygous and wild-type littermates were genotyped by Southern blot analysis. Heterozygous mice of subsequent generations were identified by PCR using a forward primer (5′-ATGGTGCGCACAGCCTACACGGTG-3′) and a reverse primer (5′-

TAGAAGGCACAGTCGAGG-3′). Animals were euthanized at 4 weeks, 2 months, and 4 months after birth for tissue harvesting. After the heads were dissected, they were immediately immersed in Bouin's fixative (0.9% picric acid, 9% v/v formaldehyde, and 5% acetic acid; Polysciences, Warrington, PA USA) for 24 hr and then transferred to 70% ethanol for histological analysis. For backscatter scanning electron microscopy (SEM), the tissues were not fixed and were stored in phosphate buffered saline (PBS) saturated with thymol. Animal experiments were approved by the Animal Care and Use Committee of Saint Francis Hospital and Medical Center and by the University of Washington committee on Use and Care of Animals in compliance with state and federal laws.

Gross Appearance and Radiographic Analysis

Head specimens from male and female gremlin OE mice at 4 weeks, 2 months, and 4 months of age were photographed using a Nikon digital camera with a 105 mm macro-lenses (D70, Nikon, Chiyodaku, Japan). The lower lips were removed to obtain optimal views of the mandibular incisors. For radiographic analysis, the head specimens were hemisected along the midline. The right halves were laid on a radiographic film (X-OMAT V Film, Kodak, Rochester, NY, USA) and exposed at 50 kV and 3 mA for 50 sec in an X-ray unit (Faxitron cabinet X-ray systems, Picker, Cleveland, OH, USA). The films were developed for analysis.

Histological Analysis

Mandibles were dissected from surrounding tissues, followed by decalcification for 2 weeks in acetic acid and normal saline (4% formaldehyde in 0.85% NaCl +10% acetic acid). Decalcification endpoint was determined by the flexibility of the mandible, and subsequently tissues were processed by dehydration in a graded ethanol series and embedded in paraffin. Buccolingual serial sections (5 μm) from 1st mandibular molars were prepared and stained with hematoxylin and eosin (H&E).

Scanning Electron Microscopy (SEM)

SEM analyses were performed on fractured incisors for microstructural characterization of enamel and polished lower 1st molars for mineral density characterization of pulp, dentin, cementum, and enamel. Incisors from 4-month-old animals were fractured approximately 1 mm from the tip of the incisor. Fractured cross sections were mounted on SEM stubs, coated with 5 nm of platinum (Pt) to achieve electron conductivity, and examined by SEM in secondary electron (SE) mode using a JSM-7000F SEM at 10 keV (Jeol-USA, Peabody, MA, USA).

For mineral density studies, extracted lower 1st molars, also from 4-month-old animals, were dehydrated sequentially in 5%, 10%, 25%, 50%, 75%, and 100% aqueous ethanol solutions for 30 min at each step. After dehydration, teeth were mounted in room-temperature-cure epoxy (Allied High Tech, Rancho Dominguez, CA, USA). After grinding with 1500 grit silicon carbide paper from the mesial surface to expose the interior of the 1st molar, 200 nm ultrasections were cut using a 2.5 mm wide and 45° angle diamond knife (Diatome, Hatfield, PA, USA) fitted on a MT 6000-XL ultramicrotome (Bal-Tec RMC, Tucson, AZ, USA). The ultramicrotomed surface of the remaining block, which was not fixed, demineralized, or stained, was coated with 5 nm of Pt and used for backscatter imaging (BSE) by SEM using also the JSM-7000F SEM at 10 keV.

Cell Culture

Primary murine dental pulp cells were isolated from tooth germs of 23 days postcoital (DPC) CD-1 mice. Briefly, the lower first molars were dissected using a stereoscope and pulp tissues were removed and minced into pieces approximately 1 mm^3. These pieces were allowed to

attach to 35 mm culture dishes in Dulbecco's Modified Eagle Medium (DMEM) supplemented with 10% (v/v) fetal bovine serum (FBS), 100 units/ml penicillin, 100 μg/ml streptomycin, and 2 mM L-glutamine. They were cultured at 37°C in 5% CO_2 until cells began to migrate from the tissue pieces (≈10 days). Cells were then trypsinized, passed to 100 mm plates, and designated as passage 0 (P0). These cells were cultured and passaged until P2, at which time they were aliquoted and stored in liquid nitrogen for further use. For in vitro experiments, cells of passage 4 were used. Cells were maintained in DMEM supplemented with 10% (v/v) FBS, 100 units/ml penicillin, 100 μg/ml streptomycin, and 2 mM L-glutamine. Tissue culture reagents were obtained from Invitrogen/GIBCO BRL (Carlsbad, CA, USA)

Mineralization Assay

To investigate the effect of BMP-4 and gremlin on odontogenic differentiation and associated mineralization, cells were plated at a density of 0.9×10^4 cells/well (24 well plates) in DMEM supplemented with 10% FBS. Upon reaching 70–80% confluence, the medium was changed to DMEM with 2% FBS and 0.3 nM BMP-4 (R&D Systems Minneapolis, MN, USA) and/or 50 nM gremlin (R&D Systems) and cultured for up to 2 weeks. Doses selected for BMP and gremlin were based on the manufacturer's recommendation and preliminary experiments. Ascorbic acid (AA, 50 μg/ml, Sigma-Aldrich, St. Louis, MO, USA) and β-glycerophosphate (β-GP, 10 mM, Sigma-Aldrich) were added to all groups to promote mineralization. Controls were cultured in 2% FBS DMEM plus 10 mM β-GP +/− 50 μg/ml AA [36]. Media were changed every 2 days during the course of the experiment. Gene expression and mineral formation were examined at 7 and 14 days after treatment. To quantitate mineralization, Alizarin red staining (AR-S, Sigma-Aldrich) was used.

Real-Time Reverse-Transcription Polymerase Chain Reaction

Total RNA was isolated using the RNeasy Micro Kit (Qiagen, Valencia, CA, USA). cDNA was prepared from 1 μg total RNA (Transcriptor kit; Roche Diagnostic, Indianapolis, IN, USA). Quantitative real-time reverse transcription polymerase chain reaction (qRT-PCR) was carried out and data analyzed as previously reported [37]. Briefly, PCR was performed for 40 cycles at 95°C for 0 sec, 55°C for 7 sec, and 72°C for 20 sec on the Lightcycler system (Roche Diagnostics, Mannheim, Germany). Genes assayed included dentin sialophosphoprotein (*Dspp*), bone sialoprotein (*Bsp*), osteopontin (*Opn*), osteocalcin (*Ocn*), with glyceraldehyde-3-phosphate dehydrogenase (*Gapdh*) serving as a housekeeping/reference gene for normalization. The sequences used for qRT-PCR are 20 μM of a forward primer (5′-AGTTCGATGACGAGTCC-3′) and of a reverse primer (5′-GTCTCTCCCGCATGT-3′) for *Dspp;* a forward primer (5′-GAGACGGCGATAGTTCC-3′) and a reverse primer (5′-AGTGCCGCTAACTCAA-3′) for *Bsp;* a forward primer (5′-*TGAACAGACTCCGGCG* -3′) and a reverse primer (5′-GATACCGTAGATGCGTTTG-3′) for *Ocn;* a forward primer (5′-TTTACAGCCTGCACCC -3′) and a reverse primer (5′-CTAGCAGTGACGGTCT -3′) for *Opn*, and a forward primer (5′-ACCACAGTCCATGCCATCAC-3′) and a reverse primer (5′-TCCACCACCCTGTTGCTGTA -3′) for *Gapdh.*

Statistical Analysis

Results are expressed as mean ± SD. One-way analysis of variance (ANOVA) followed by Tukey-Kramer's post-hoc test was performed, using Sigmastat 3.1 (Systat Software, Point Richmond, CA, USA) to determine significance among treatment groups. A difference between experimental groups was considered to be significant at $p < 0.05$.

RESULTS

Ex Vivo; Gross Appearance

The maxillary and mandibular incisors obtained from gremlin OE mice and wild-type controls were first examined macroscopically (Figure 1A). The most dramatic observation was the abnormal color of both maxillary and mandibular incisors in gremlin OE mice compared with wild-type controls. This indicated a reduction in enamel/dentin thickness, and/or a reduced degree of mineralization in enamel and/or dentin, which may be related to tooth fragility as previously reported [35]. The space between mandibular incisors in gremlin OE mice was wider than in wild-type controls, possibly resulting from occlusal forces. These differences were more prominent in the mandibular incisors, where the pulp was more visible through the translucent enamel/dentin layers compared with the maxillary incisors.

Radiographic Analysis

The observation that gremlin OE mice have more curved maxillary and mandibular incisors was confirmed by radiographs (Figure 1B). In lower incisors from gremlin OE mice, the surface of the teeth on the labial side exhibited a higher degree of radiolucency than in wild-type controls, indicating enamel and dentin mineralization defects (Figure 1C 4 weeks, 1D 4 months arrowheads, respectively). Further, the pulp chambers in molars from 4-week-old gremlin OE showed significant enlargement compared with wild-type controls (Figure 1C, right panel). The tips of the incisors of gremlin OE mice demonstrated a blunt-end as a result of periodic trimming in an effort to prevent malocclusion and malnutrition [35].

Notably, molars of 4-month-old gremlin OE mice exhibited changes in the periodontia compared with wild-type controls, with distinct radiographic signs of alveolar bone resorption at the root apex (Figure 1D, right panel, arrow). There was no apparent difference in tooth shape and size between wild-type and gremlin OE mice, suggesting that the interactions of BMPs and gremlin have no effect on tooth pattern formation.

Histological/SEM Analysis

Molars—At 4 weeks, the dental pulp chamber was expanded, dentin width was significantly decreased, and ectopic calcification was observed within the pulp chamber of gremlin OE mice (Figure 2A). These findings corresponded with the gross appearance observations and radiographic analyses (Figure 1). We noted that molars from gremlin OE mice exhibited a more severe phenotype in the radicular region than in the crown region. Moreover, the root apex started to show signs of inflammation at 4 weeks of age (Figure 2A, Gremlin, arrow). A higher magnification image of the pulp from the gremlin OE mice demonstrated that the ectopic matrix was bone-like, rather than the characteristic tubular appearance of dentin (Figure 2A, Gremlin, enlarged image, asterisk), and the dentin-pulp border was ill-defined compared with that of wild-type controls.

At 2 and 4 months, necrotic pulp cells were now observed within the radicular pulp chamber in the apical region (Figure 2B enlarged image, arrow and 2C panel C_2, arrow). The most dramatic change was the extension of the inflammation into the periodontal (PDL) region resulting in the disruption of the PDL in the apical region (Figure 2B and 2C, Gremlin). Neutrophils were the major cell type noted with a few lymphocytes and plasma cells present (Figure 2C, panel C_4). Further, the PDL region exhibited a decrease in cellularity compared with the WT (Figure 2B, enlarged images). No differences were noted in cementum and alveolar bone between gremlin OE and wild-type mice at all time points (Figures 2A, 2B, and 2C).

Figure 3 provides data on the characteristics of the molar tissues using BSE. In this technique, greater numbers of backscattered electrons are generated in regions with higher mineral density, which corresponds to a brighter appearance in the images. As shown in Figure 3, enamel, the most mineralized tissue, appeared the most reflective, while the less mineralized dentin and bone appeared less bright, and nonmineralized pulp, PDL, and surrounding epoxy appeared darkest. BSE analysis of longitudinal sections from gremlin OE and wild-type molars, respectively, revealed that the amount of intact enamel in the gremlin OE mice (Figure 3, Gremlin) was less than that in wild-type (WT) (Figure 3, WT). A zoom-in image of the cervical root revealed that the mineralized matrix within the pulp region in the gremlin OE mice (Figure 3, Gremlin, enlarged image) was similar to bone, containing cells resembling osteocytes.

Incisors—In rodent incisors, enamel forms exclusively on the labial surface, and their enamel-free lingual surface is considered to be the root analogue [38–40]. Mandibular incisors of gremlin OE mice were examined at ages of 4 weeks, 2 months (data not shown), and 4 months (Figure 4). The phenotype described above for molars was also apparent for incisors, i.e. thin dentin and altered pulp chambers compared with wild-type controls (Figure 4A). The ameloblasts were less polarized in incisors from gremlin OE mice compared with those from wild-type. These observations suggest that ameloblast maturation was delayed in gremlin OE mice. Similar findings were noted for odontoblasts on the labial side with lack of polarization and the absence of columnar shape compared with those on the lingual side from the same transgenic mice and wild-type (data not shown for WT odontoblasts and lingual side of odontoblasts from Gremlin). This observation suggests that maturation of odontoblasts on the labial side was inhibited.

SEM investigation of enamel from incisors of gremlin OE mice revealed a dramatic defect in crystal formation with no recognizable rod structure, suggestive of a form of amelogenesis imperfecta resulting from delayed maturation of ameloblasts (Figure 4B, right panel). In contrast, the clear deccusation of enamel rods was seen in samples from wild-type incisors (Figure 4B, left panel).

In vitro; Mineralization Assay—To assess the effect of excess gremlin on the accumulation of mineral by pulp cells, Alizarin red staining was carried out after 7 and 14 days in culture (day 7; data not shown, day 14; Figures 5A and 5B) with addition of BMP-4 and/or gremlin, in the presence of 10 mM β-GP +/−50 μg/ml AA. In positive control samples, i.e. 10 mM β-GP + 50 μg/ml AA, mineral formation was noted by 14 days. In contrast, no mineral formation was noted in negative control pulp cells (-AA) (data not shown). In the presence of BMP-4, pulp cells promoted mineral formation by day 7 with continuous mineral formation through the period assayed. Increased matrix mineralization induced by BMP-4 was significantly blocked by 50 nM gremlin, while gremlin alone did not inhibit mineral deposition in cells treated with AA+β-GP (Figure 5B).

Effect of BMP-4 and Gremlin on Gene Expression

To analyze gene expression associated with mineral formation, the levels of mRNA for *Dspp* were examined by qRT-PCR at day 14. In the presence of BMP-4, *Dspp* was increased 3 fold over control cells, while gremlin blocked this increase (Figure 5C). Gremlin alone has no effects on *Dspp* expression beyond that noted for control cells. There were no significant differences in the level of *Bsp, Ocn*, and *Opn* mRNA expression between BMP-4 treated cells and all other conditions (data not shown).

DISCUSSION

A previous study characterizing gremlin OE mice reported a decrease in body size, an increase in cortical bone width, and a decrease in trabecular bone volume, resulting in spontaneous fractures and modeling defects of long bones [35]. The data here provide new insights into the importance of BMP agonist and antagonist interactions during odontogenesis/cytodifferentiation.

Our findings demonstrate that transgenic mice overexpressing the BMP antagonist gremlin, under the control of the osteocalcin promoter, develop teeth exhibiting enlarged pulp chambers with ectopic calcification of the pulp, thin dentin and enamel, and inflammation surrounding the root apex, resulting in periodontal pathology. In vitro studies revealed that gremlin inhibited BMP-4-mediated induction of *Dspp* in murine pulp cells. Molars from gremlin OE mice exhibited a more severe dentin phenotype in the radicular region than in the crown region (Figures 2A, 2B, and 2C).

A number of studies suggest that the signaling pathways associated with crown formation are different from those required for root formation, and our findings support this hypothesis. For example, Six et al. [41], using rat molars, examined the ability of BMP-7 to induce reparative dentinogenesis after pulp exposure and found that reparative dentin in the radicular portion was comprised of homogeneous mineralized tissue characterized by a tubular structure, while porous heterogeneous osteodentin was seen in the coronal region. Although the exact time of transgenic expression of gremlin in the teeth of mice was not determined, its expression of osteocalcin in teeth, used to direct gremlin overexpression, starts at E18.5, i.e., in late bell stage in mature columnar odontoblasts [42]. Thus, it is reasonable to suggest that gremlin expression was initiated by E18.5, and as a result, radicular dentin was more severely affected than crown dentin.

Gremlin OE Mice Incisors Exhibited Enamel Defect

The disruption of ameloblast maturation in gremlin OE mice is not surprising. Several studies have demonstrated the importance of interactions between BMP agonists and antagonists for proper crown development [8,2]. Noggin is known to bind to and antagonize BMP-2, -4, and -7, with higher affinity for BMP-2 and -4 [43]. It has also been shown that follistatin binds to BMP-2, -4, and -7, with higher affinity for BMP-7 [44,45]. These differences in affinity for the various BMPs may explain the different phenotypes for mice overexpressing a specific BMP antagonist. For example, follistatin, a known antagonist of TGF-β signaling, inhibits activin and BMP-mediated signaling [46]. Ameloblasts do not differentiate in K14-follistatin overexpressing mice.

Work by Plikus et al. [3] demonstrated that overexpressing noggin keratin 14 (K14) in the oral and dental epithelium prevented maturation of both ameloblasts and odontoblasts. Although layers of dentin-like material eventually formed, these deposits were irregular, resulting in markedly defective dentin in a similar fashion to noggin.

Therefore, we propose that gremlin overexpression inhibited BMP-mediated signaling from preodontoblasts/odontoblasts to preameloblast/ameloblasts, altering ameloblast development and resulting in defective enamel crystal deposition (Figure 4B).

Periodontal Pathology

From 4 weeks to 4 months, gremlin OE exhibited an increase in the degree of inflammation at the root apex. We speculate that this response was induced by pulp necrosis rather than a direct effect of gremlin on PDL cells.

In Vitro Results

Histological and SEM analysis of first molars from gremlin OE mice revealed bone-like mineralized tissue in the pulp chambers (Figures 2 and 3). In vitro studies explored the regulatory mechanisms which contribute to this phenotype. *Dspp*, a protein belonging to the SIBLING family (Small Integrin Binding Ligand N-linked Glycoprotein), is highly selective to odontoblasts. The effect of gremlin on *Dspp* expression in pulp cells was determined in murine dental pulp cells in vitro. The importance of *Dspp* in dentinogenesis has been demonstrated by the observations that mutations in the *Dspp* gene are associated with dentinogenesis imperfecta in humans [47], and *Dspp* gene knockout mice show hypomineralization of dentin (widening of predentin) [48]. Transgenic mice overexpressing active TGF-β1 driven by the *Dspp* promoter, displayed decreased mineralization of enamel and dentin, abnormal dentin formation, and downregulated *Dspp* mRNA expression [49].

While highly speculative, it is possible to consider that the ectopic mineralized pulp tissues observed in the transgenic mice result from the ability of gremlin to downregulate *Dspp*, ultimately driving pulp cells toward an osteoblast rather than an odontoblast phenotype. In support of this, subcutaneously transplanted pulp cells were shown to form a mineralized matrix possessing bone- or cementum-like characteristics, suggesting that pulp cells are capable of forming "osteogenic" versus "dentinogenic" tissues, depending on the microenvironmental cues presented to the cells [50]. Further studies are needed to clarify the specific molecules regulating the formation of dentin versus bone or cementum and would include the exposure of pulp cells and PDL cells to multiple BMP agonists and antagonists.

CONCLUSION

These data substantiate existing evidence that balanced interactions between BMP agonists/antagonists are required for proper development of teeth and surrounding tissues. The profound effects that these factors have on tooth development highlight the sensitivity of cells associated with tooth and supporting structures to these stimuli and thus the potential to use such factors for regeneration of these tissues. Nevertheless, it is clear that these interactions are complex and require further investigation to better define the mechanisms controlling tooth root formation (pulp, dentin, cementum, and surrounding tissue) to provide the information needed to successfully regenerate these tissues.

Acknowledgments

The authors thank Erica C. Swanson, Daisy Matsa Dunn, and Kuang-Dah Yeh for their assistance. This work was supported by NIH/NIDCR Grant DE09532, and NIH/NIAMS Grant AR021707.

References

1. Canalis E, Economides AN, Gazzerro E. Bone morphogenetic proteins, their antagonists, and the skeleton. Endocr Rev 2003;24:218–235. [PubMed: 12700180]
2. Kassai Y, Munne P, Hotta Y, Penttila E, Kavanagh K, Ohbayashi N, Takada S, et al. Regulation of mammalian tooth cusp patterning by ectodin. Science 2005;309:2067–2070. [PubMed: 16179481]
3. Plikus MV, Zeichner-David M, Mayer JA, Reyna J, Bringas P, Thewissen JG, Snead ML, et al. Morphoregulation of teeth: Modulating the number, size, shape and differentiation by tuning Bmp activity. Evol Dev 2005;7:440–457. [PubMed: 16174037]
4. Thesleff I. Epithelial-mesenchymal signalling regulating tooth morphogenesis. J Cell Sci 2003;116:1647–1648. [PubMed: 12665545]
5. Urist MR. Bone: Formation by autoinduction. Science 1965;150:893–899. [PubMed: 5319761]

6. Wang XP, Suomalainen M, Jorgez CJ, Matzuk MM, Werner S, Thesleff I. Follistatin regulates enamel patterning in mouse incisors by asymmetrically inhibiting BMP signaling and ameloblast differentiation. Dev Cell 2004;7:719–730. [PubMed: 15525533]
7. Peters H, Balling R. Teeth. Where and how to make them. Trends Genet 1999;15:59–65. [PubMed: 10098408]
8. Aberg T, Wozney J, Thesleff I. Expression patterns of bone morphogenetic proteins (Bmps) in the developing mouse tooth suggest roles in morphogenesis and cell differentiation. Dev Dyn 1997;210:383–396. [PubMed: 9415424]
9. Bitgood MJ, McMahon AP. Hedgehog and Bmp genes are coexpressed at many diverse sites of cell-cell interaction in the mouse embryo. Dev Biol 1995;172:126–138. [PubMed: 7589793]
10. Heikinheimo K. Stage-specific expression of decapentaplegic-Vg-related genes 2, 4, and 6 (bone morphogenetic proteins 2, 4, and 6) during human tooth morphogenesis. J Dent Res 1994;73:590–597. [PubMed: 8163729]
11. Helder MN, Karg H, Bervoets TJ, Vukicevic S, Burger EH, D'Souza RN, Woltgens JH, et al. Bone morphogenetic protein-7 (osteogenic protein-1, OP-1) and tooth development. J Dent Res 1998;77:545–554. [PubMed: 9539457]
12. Helder MN, Ozkaynak E, Sampath KT, Luyten FP, Latin V, Oppermann H, Vukicevic S. Expression pattern of osteogenic protein-1 (bone morphogenetic protein-7) in human and mouse development. J Histochem Cytochem 1995;43:1035–1044. [PubMed: 7560881]
13. Lyons KM, Hogan BL, Robertson EJ. Colocalization of BMP 7 and BMP 2 RNAs suggests that these factors cooperatively mediate tissue interactions during murine development. Mech Dev 1995;50:71–83. [PubMed: 7605753]
14. Nadiri A, Kuchler-Bopp S, Haikel Y, Lesot H. Immunolocalization of BMP-2/-4, FGF-4, and WNT10b in the developing mouse first lower molar. J Histochem Cytochem 2004;52:103–112. [PubMed: 14688221]
15. Thesleff I, Keranen S, Jernvall J. Enamel knots as signaling centers linking tooth morphogenesis and odontoblast differentiation. Adv Dent Res 2001;15:14–18. [PubMed: 12640732]
16. Vaahtokari A, Aberg T, Jernvall J, Keranen S, Thesleff I. The enamel knot as a signaling center in the developing mouse tooth. Mech Dev 1996;54:39–43. [PubMed: 8808404]
17. Yamashiro T, Tummers M, Thesleff I. Expression of bone morphogenetic proteins and Msx genes during root formation. J Dent Res 2003;82:172–176. [PubMed: 12598544]
18. Bahamonde ME, Lyons KM. BMP3: to be or not to be a BMP. J Bone Joint Surg 2001;83-A(Suppl 1):S56–62. [PubMed: 11263666]
19. Gamer LW, Nove J, Levin M, Rosen V. BMP-3 is a novel inhibitor of both activin and BMP-4 signaling in Xenopus embryos. Dev Biol 2005;285:156–168. [PubMed: 16054124]
20. Gagari, E. BMP-3 overexpression results in dentin and periodontal ligament defects. Abstract. IADR Conference; Orlando, FL. 2006.
21. Iohara K, Nakashima M, Ito M, Ishikawa M, Nakasima A, Akamine A. Dentin regeneration by dental pulp stem cell therapy with recombinant human bone morphogenetic protein 2. J Dent Res 2004;83:590–595. [PubMed: 15271965]
22. Nakashima M, Nagasawa H, Yamada Y, Reddi AH. Regulatory role of transforming growth factor-beta, bone morphogenetic protein-2, and protein-4 on gene expression of extracellular matrix proteins and differentiation of dental pulp cells. Dev Biol 1994;162:18–28. [PubMed: 8125185]
23. Saito T, Ogawa M, Hata Y, Bessho K. Acceleration effect of human recombinant bone morphogenetic protein-2 on differentiation of human pulp cells into odontoblasts. J Endodont 2004;30:205–208.
24. Vainio S, Karavanova I, Jowett A, Thesleff I. Identification of BMP-4 as a signal mediating secondary induction between epithelial and mesenchymal tissues during early tooth development. Cell 1993;75:45–58. [PubMed: 8104708]
25. Nakashima M. Induction of dentin formation on canine amputated pulp by recombinant human bone morphogenetic proteins (BMP)-2 and -4. J Dent Res 1994;73:1515–1522. [PubMed: 7929986]
26. Nakashima M. Induction of dentine in amputated pulp of dogs by recombinant human bone morphogenetic proteins-2 and -4 with collagen matrix. Arch Oral Biol 1994;39:1085–1089. [PubMed: 7717891]

27. Rutherford RB, Gu K. Treatment of inflamed ferret dental pulps with recombinant bone morphogenetic protein-7. Euro J Oral Sci 2000;108:202–206.
28. Rutherford RB, Spangberg L, Tucker M, Rueger D, Charette M. The time-course of the induction of reparative dentine formation in monkeys by recombinant human osteogenic protein-1. Arch Oral Biol 1994;39:833–838. [PubMed: 7741652]
29. Rutherford RB, Wahle J, Tucker M, Rueger D, Charette M. Induction of reparative dentine formation in monkeys by recombinant human osteogenic protein-1. Arch Oral Biol 1993;38:571–576. [PubMed: 8368953]
30. Pummila M, Fliniaux I, Jaatinen R, James MJ, Laurikkala J, Schneider P, Thesleff I, Mikkola ML. Ectodysplasin has a dual role in ectodermal organogenesis: Inhibition of Bmp activity and induction of Shh expression. Development 2007;134:117–125. [PubMed: 17164417]
31. Hsu DR, Economides AN, Wang X, Eimon PM, Harland RM. The Xenopus dorsalizing factor Gremlin identifies a novel family of secreted proteins that antagonize BMP activities. Mol Cell 1998;1:673–683. [PubMed: 9660951]
32. Pereira RC, Economides AN, Canalis E. Bone morphogenetic proteins induce gremlin, a protein that limits their activity in osteoblasts. Endocrinology 2000;141:4558–4563. [PubMed: 11108268]
33. Nakamura Y, Wakitani S, Nakayama J, Wakabayashi S, Horiuchi H, Takaoka K. Temporal and spatial expression profiles of BMP receptors and noggin during BMP-2-induced ectopic bone formation. J Bone Miner Res 2003;18:1854–1862. [PubMed: 14584896]
34. Sun J, Zhuang FF, Mullersman JE, Chen H, Robertson EJ, Warburton D, Liu YH, Shi W. BMP4 activation and secretion are negatively regulated by an intracellular gremlin-BMP4 interaction. J Biol Chem 2006;281:29349–29356. [PubMed: 16880207]
35. Gazzerro E, Pereira RC, Jorgetti V, Olson S, Economides AN, Canalis E. Skeletal overexpression of gremlin impairs bone formation and causes osteopenia. Endocrinology 2005;146:655–665. [PubMed: 15539560]
36. Liu J, Jin T, Chang S, Ritchie HH, Smith AJ, Clarkson BH. Matrix and TGF-beta-related gene expression during human dental pulp stem cell (DPSC) mineralization. In Vitro Cell Develop Biol 2007;43:120–128.
37. Foster BL, Nociti FH Jr, Swanson EC, Matsa-Dunn D, Berry JE, Cupp CJ, Zhang P, Somerman MJ. Regulation of Cementoblast gene expression by inorganic phosphate in vitro. Calcified Tis Inter 2006;78:103–112.
38. Amar S, Karcher-Djuricic V, Meyer JM, Ruch JV. The lingual (root analogue) and the labial (crown analogue) mouse incisor dentin promotes ameloblast differentiation. Arch D'anat Microscop De Morphol Exper 1986;75:229–239.
39. Amar S, Luo W, Snead ML, Ruch JV. Amelogenin gene expression in mouse incisor heterotopic recombinations. Differentiation, Res Biolog Diversity 1989;41:56–61.
40. Tummers M, Thesleff I. Root or crown: a developmental choice orchestrated by the differential regulation of the epithelial stem cell niche in the tooth of two rodent species. Development 2003;130:1049–1057. [PubMed: 12571097]
41. Six N, Lasfargues JJ, Goldberg M. Differential repair responses in the coronal and radicular areas of the exposed rat molar pulp induced by recombinant human bone morphogenetic protein 7 (osteogenic protein 1). Arch Oral Biol 2002;47:177–187. [PubMed: 11839353]
42. Bidder M, Latifi T, Towler DA. Reciprocal temporospatial patterns of Msx2 and Osteocalcin gene expression during murine odontogenesis. J Bone Miner Res 1998;13:609–619. [PubMed: 9556061]
43. Zimmerman LB, De Jesus-Escobar JM, Harland RM. The Spemann organizer signal noggin binds and inactivates bone morphogenetic protein 4. Cell 1996;86:599–606. [PubMed: 8752214]
44. Iemura S, Yamamoto TS, Takagi C, Uchiyama H, Natsume T, Shimasaki S, Sugino H, Ueno N. Direct binding of follistatin to a complex of bone-morphogenetic protein and its receptor inhibits ventral and epidermal cell fates in early Xenopus embryo. Proc Nat Acad Sci USA 1998;95:9337–9342. [PubMed: 9689081]
45. Yamashita H, ten Dijke P, Huylebroeck D, Sampath TK, Andries M, Smith JC, Heldin CH, Miyazono K. Osteogenic protein-1 binds to activin type II receptors and induces certain activin-like effects. J Cell Biol 1995;130:217–226. [PubMed: 7790373]

46. Balemans W, Van Hul W. Extracellular regulation of BMP signaling in vertebrates: A cocktail of modulators. Dev Biol 2002;250:231–250. [PubMed: 12376100]

47. Zhang X, Zhao J, Li C, Gao S, Qiu C, Liu P, Wu G, et al. DSPP mutation in dentinogenesis imperfecta Shields type II. Nat Genet 2001;27:151–152. [PubMed: 11175779]

48. Sreenath T, Thyagarajan T, Hall B, Longenecker G, D'Souza R, Hong S, Wright JT, et al. Dentin sialophosphoprotein knockout mouse teeth display widened predentin zone and develop defective dentin mineralization similar to human dentinogenesis imperfecta type III. J Biol Chem 2003;278:24874–24880. [PubMed: 12721295]

49. Thyagarajan T, Sreenath T, Cho A, Wright JT, Kulkarni AB. Reduced expression of dentin sialophosphoprotein is associated with dysplastic dentin in mice overexpressing transforming growth factor-beta 1 in teeth. J Biol Chem 2001;276:11016–11020. [PubMed: 11116156]

50. Hosoya A, Nakamura H, Ninomiya T, Hoshi K, Yoshiba K, Yoshiba N, Takahashi M, et al. Hard tissue formation in subcutaneously transplanted rat dental pulp. J Dent Res 2007;86:469–474. [PubMed: 17452570]

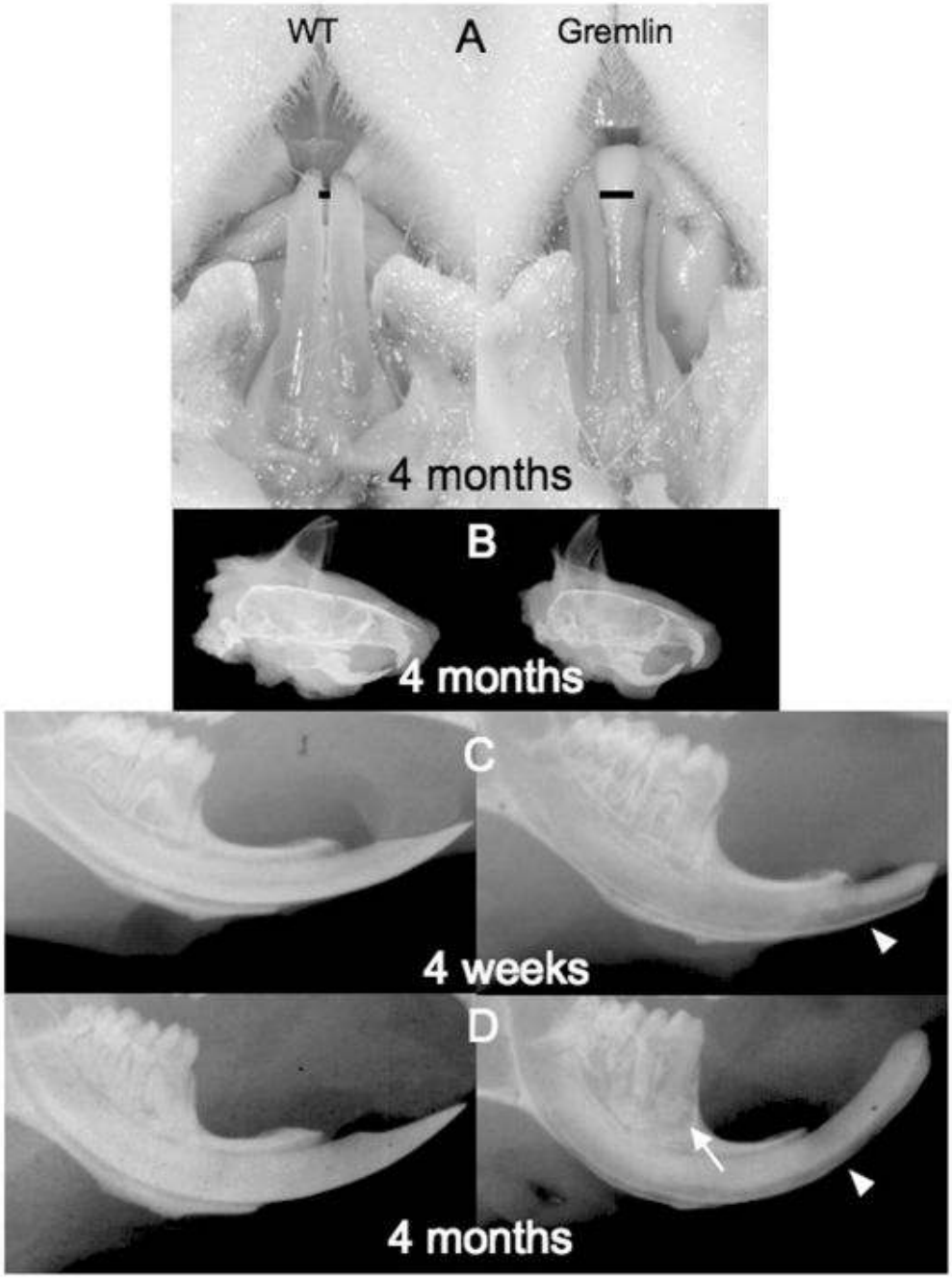

FIG. 1.

Gross appearance and radiographic analysis. (A) 4-month-old male Gremlin OE mouse (right panel) has pulp tissue visible through lower incisors. Also note widened space (black bar) between lower incisors in Gremlin versus. Wild type(WT) mouse. (B) Lateral cephalic view of 4-month-old male WT (left) and Gremlin (right) mice. Note the excessive curvature of upper and lower incisors of the Gremlin mouse. (C, D) Lower mandible radiographic examination, WT (left) Gremlin (right), 4 weeks (C), and 4 months (D). The pulp chamber in molars from 4 weeks Gremlin (C, right) showed significant enlargement compared with WT (C, left). Labial surface of Gremlin incisor is more radiolucent (C, D white arrowhead) and molars exhibit periapical alveolar bone resorption (D, white arrow).

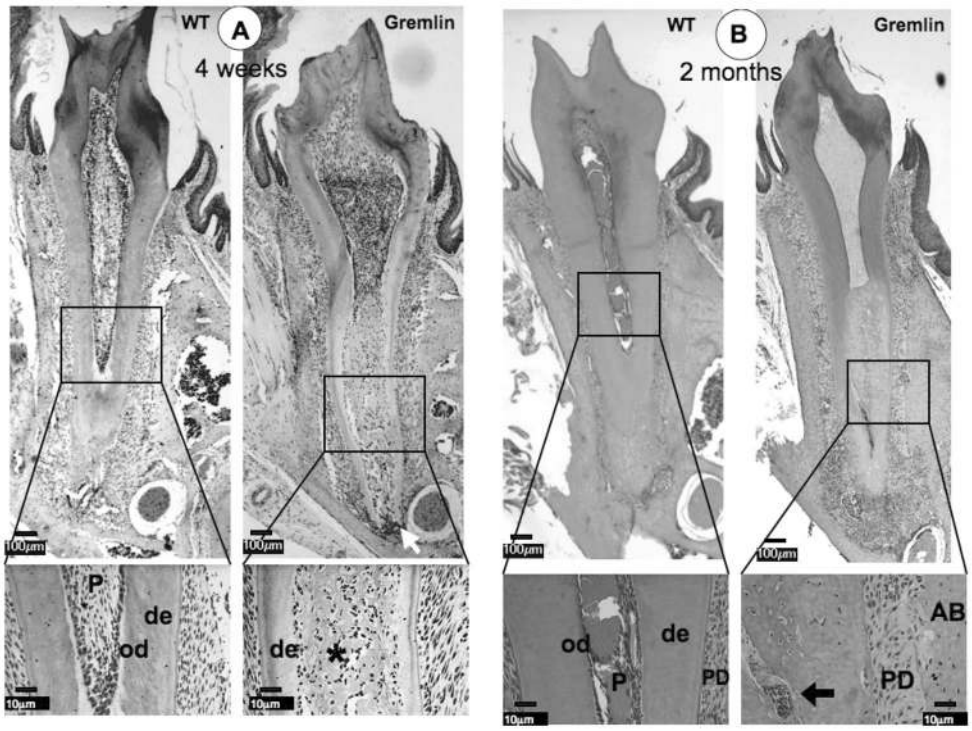

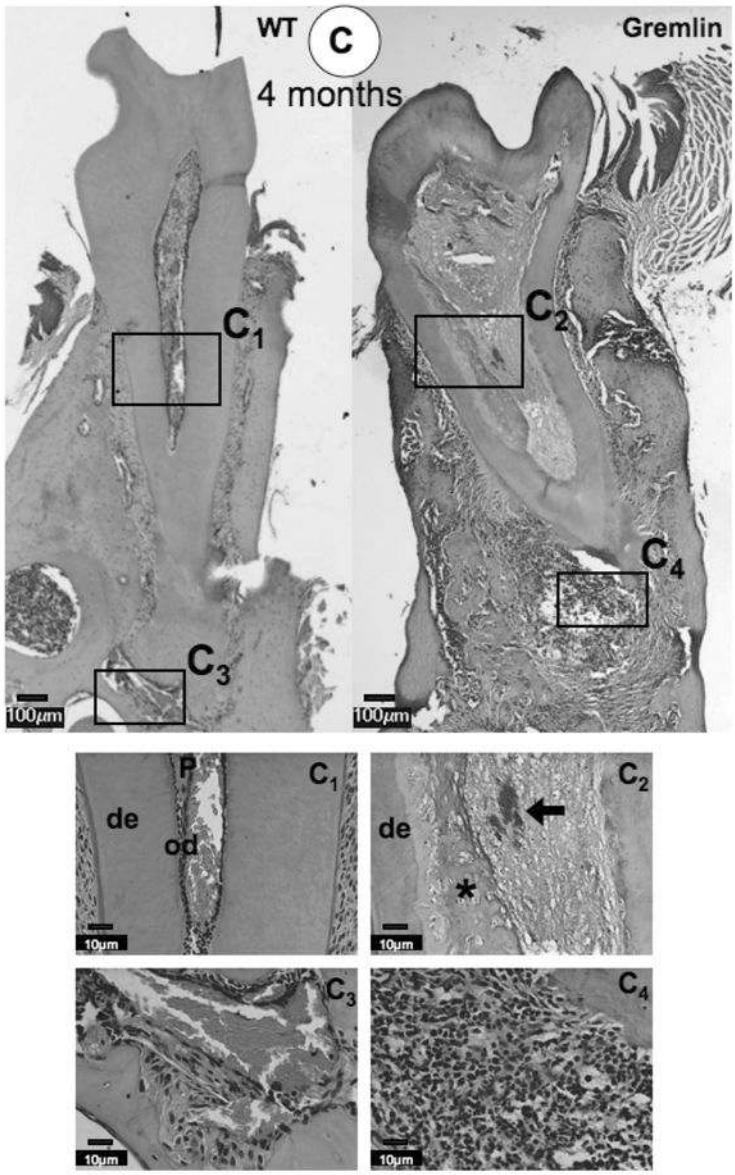

FIG. 2.

Histological analysis at 4 weeks (A), 2 months (B), and 4 months (C) of age. (A) At 4 weeks, ectopic calcification with entrapped cells is visible in the pulp space of the Gremlin mice (asterisk), which is seen as a tubular in nature in the enlarged view. Inflammation is seen at the Gremlin root apex (white arrow). The WT mouse pulp space is seen as normal. (B) Similar pulpal morphology is seen at 2 months, but with more extensive necrotic cells noted in root pulp (see enlarged view, arrow), with continued apical inflammation. Further, the PDL space of the Gremlin mouse appears to be much less cellular (see enlarged view Gremlin mouse). (C) As noted at earlier time points, 4 month Gremlin mouse pulp contains mineralized tissue with entrapped cells with extensive apical inflammation. C1–C4 Higher magnification of 4-month-old mice pulp and apical regions. C1 = Normal appearance of WT pulp and C2 = Entrapped cells in Gremlin mouse pulp (asterisk) with necrotic cells noted (black arrow). C3 = Periapical region of WT is normal in appearance. C4 = High degree of inflammation at the apex of Gremlin mainly composed of neutrophils, but lymphocytes and plasma cells are also

present. Scale bars = 100 μm in whole molar images, 10 μm in enlarged images. De = dentin, od = odontoblasts, P = pulp, PD = periodontal ligament, AB = alveolar bone.

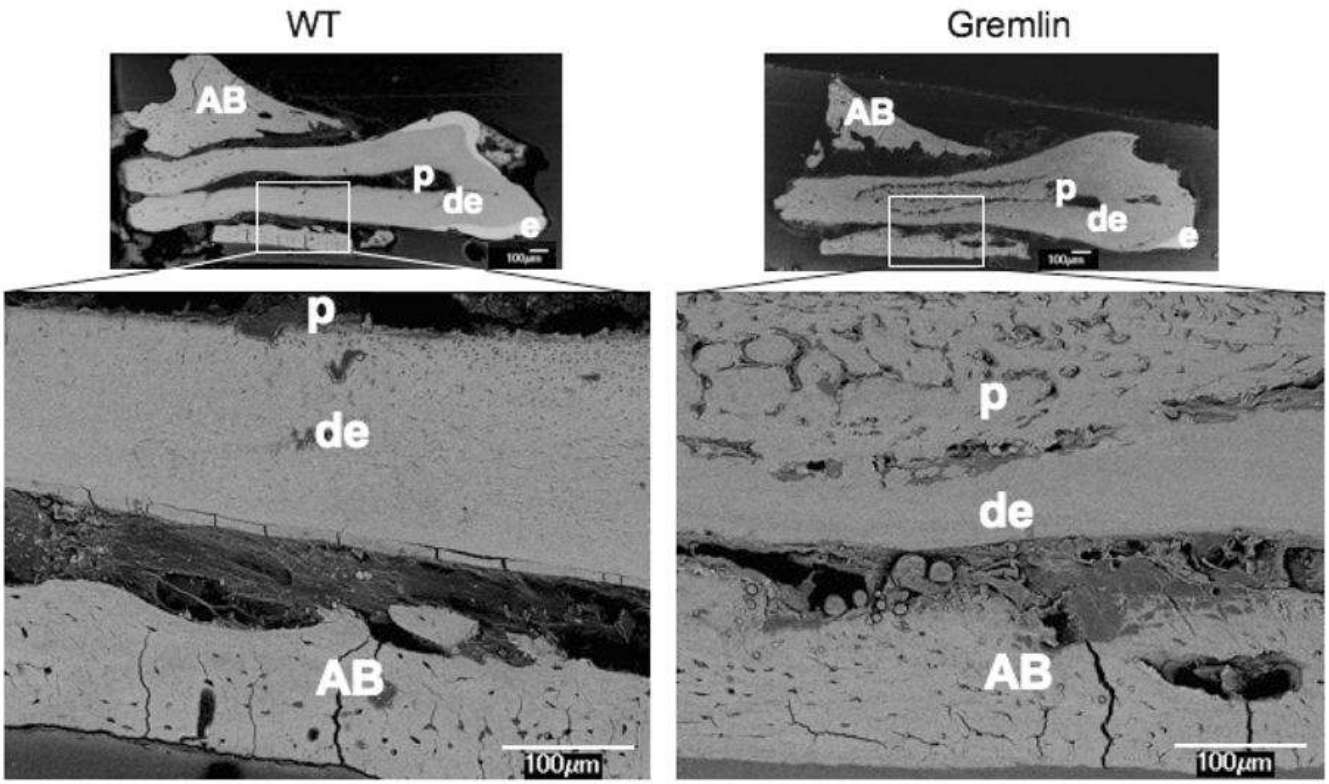

FIG. 3.

Backscatter mode scanning electron microscopy (SEM) image at age of 4 months old 1st molars in the left mandible. WT (left) mouse shows normal appearance of dentin (de), enamel (e), and pulp chamber (p). Gremlin mouse (right) molar exhibits thinner enamel with mineralized tissue in the pulp chamber. At higher magnification the mineral tissue appear bone-like, and also its presence results in diminished thickness of root dentin. Scale bars = 100 μm, AB = alveolar bone.

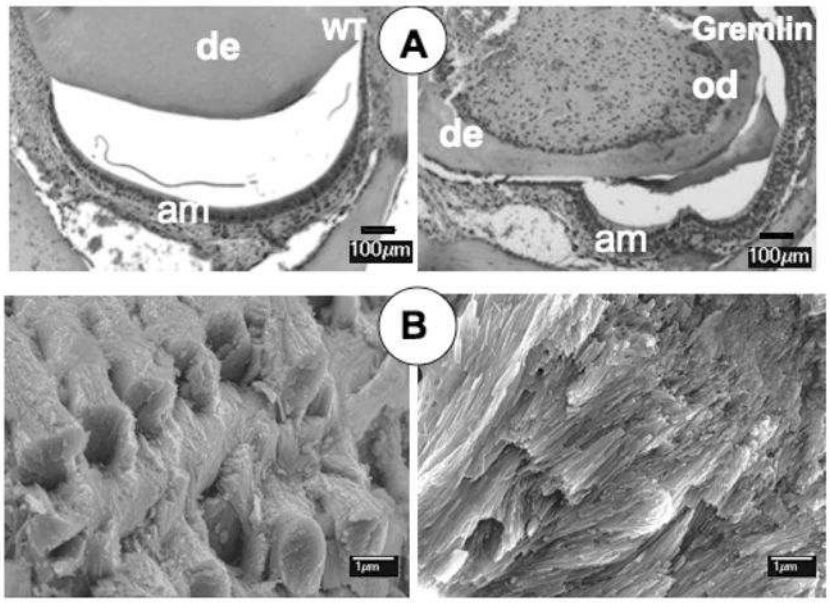

FIG. 4.

Histological and SEM analysis of 4 month lower incisors. (A) WT (left) has normal dentin thickness and labial enamel space with well-polarized ameloblasts observed. Gremlin OE mouse incisor (right) has much thinner dentin, and the enamel space is constricted mesiodistally with some ameloblasts lacking polarity. Scale bars = 100 μm, am = ameloblasts, de = dentin, od = odontoblasts. (B) SEM of WT enamel (left) shows characteristic weaved pattern of enamel crystal rods interpacked with interrod crystals. Gremlin enamel (right) lacks proper rod-interrod packing structure. Scale bars = 1 μm.

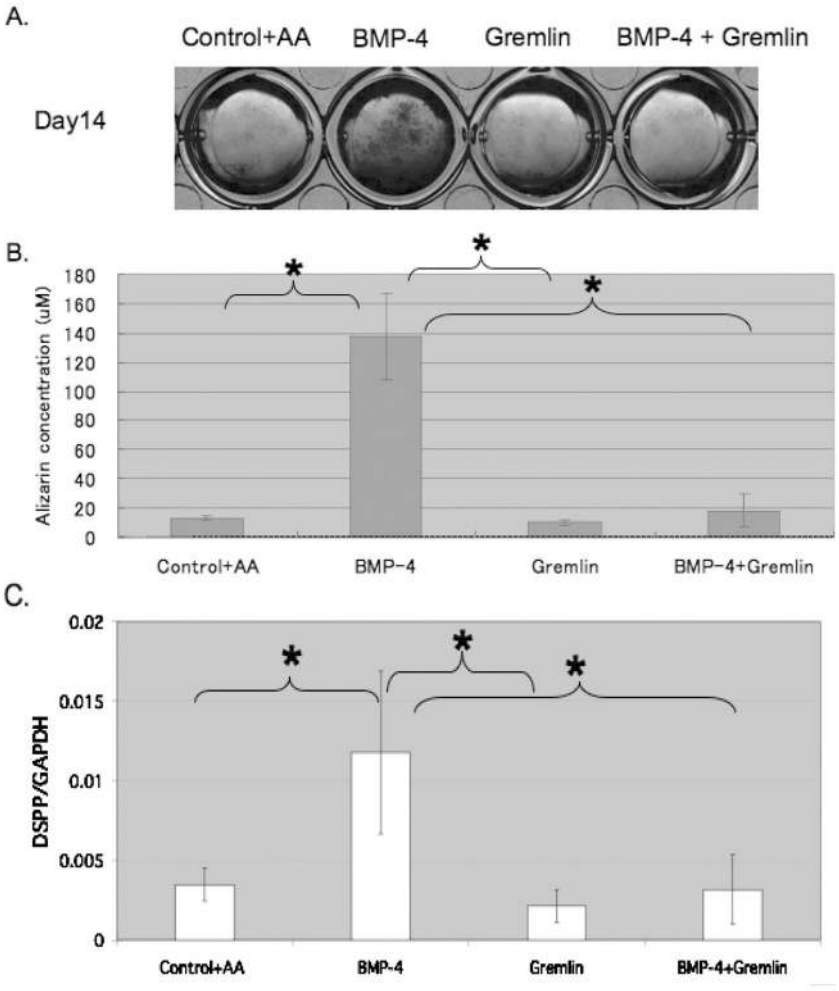

FIG. 5.

In vitro 14 days mineralization and gene expression assays using murine dental pulp (DP) cells. (A) In vitro Alizarin red staining assay for calcium precipitation with murine dental pulp cells treated with β-GP. Significant staining is seen in cells treated with BMP-4, with minimal staining in control cells and cells treated with both BMP-4 and gremlin or gremlin alone. (B) Quantification of staining in (A) above shows significant differences between BMP-4 treated cells and all other conditions, $p < 0.05$. (C) Quantitative RT-PCR analysis of *Dspp* mRNA expression in DP cells. DP cells treated with BMP-4 had significantly higher *Dspp* expression compared with other treatment groups or control cells, $p < 0.05$.